JOURNAL OF APPLIED ELECTROCHEMISTRY 24 (1994) 906–910

Nucleation and growth of copper on glassy carbon and steel

L. BONOU, M. EYRAUD, J. CROUSIER

Laboratoire de Physico-Chimie des Matériaux, Equipe Corrosion et Electrochimie. Université de Provence, Place Victor Hugo, 13331 Marseille, Cedex 3, France

Received 13 March 1993; revised 10 January 1994

The nucleation and growth of copper from sulphate solution have been studied on two substrates, glassy carbon and stainless steel. Investigations were performed by linear sweep voltammetry, potential and current step methods. The results suggest that a copper coating is formed on glassy carbon by three-dimensional nucleation and growth of the crystallites up to coalescence. On steel, after the formation of crystallites by the same mechanism as above, a second step was observed. The oxide layer, which was on the parts of the substrate not covered by the first crystallites, was reduced, allowing copper to deposit on the renewed surface by a non-nucleated process. This may explain the rapid covering of steel, as compared with the slow covering of glassy carbon, and the different morphology of the deposits obtained on the two substrates.

1. Introduction

Nucleation and growth in metal deposition depend primarily on the nature of the plating bath. The presence of free or complex cations, the pH of the bath and the hydrodynamic conditions are important factors which have been widely studied. The substrate, onto which the electrochemical reduction is performed, is also a significant parameter, not only because of its chemical nature, but also its structural state. The nucleation process is closely related to the active sites existing on the substrate, because with the same bath, and the same experimental conditions, different deposits can be obtained by using various substrates. Hydrogen evolution, either on the substrate or on the first crystallites of the deposit, must also be considered. Although copper deposits have been widely used to form thin and thick coatings [1–6], relatively few experiments have been conducted to study the first stages of deposition and the role of the chemical nature on the morphology of the deposit.

This paper describes a study of the early stages of electrocrystallization from copper sulphate solution on two substrates. The selected substrates present the necessary qualities to obtain an interesting comparison. Vitreous carbon is amorphous, presents poor interaction with metallic deposits, and has a high overpotential for hydrogen evolution. Stainless steel is polycrystalline, presents better interaction with metallic deposits, and has a lower overpotential for hydrogen evolution.

2. Experimental details

A classic three-electrode cell was used. The substrates were glassy carbon, referred to as GC (Tokaï, cross-section of a 3 mm diameter rod), and stainless steel (UR B6 from Creusot-Loire, 8 mm diameter rod), embedded in resin. After polishing with diamond paste, the electrodes were ultrasonically cleaned for one minute and then immersed in the plating bath without drying. The counter electrode was a platinum sheet, and all the potentials are referred to a saturated calomel electrode (SCE).

The sulphate solution, 0.0 M copper sulphate in 0.5 M sodium sulphate, was prepared with water treated by a millipore system. The solution was deaerated by bubbling pure argon gas before the experiments, and then an argon blanket was maintained over the surface. No agitation was provided during the experiments, except when specified.

The equipment consisted of a PAR model 273 potentiostat, using a microcomputer system (IBM-AT), capable of both controlling the experiments, and collecting and plotting the data. The electrochemical methods used were linear sweep voltammetry and potential and current step polarisations. The potential sweeps of steps started from the rest potential of the substrate in the solution considered, going in the cathodic direction.

The surface morphology of the deposits was examined using optical and scanning electron microscopy (SEM). Chemical analysis of the surface was performed by energy dispersive spectrometry (EDS).

3. Results and discussion

3.1. *Linear sweep voltammetry*

Before running the electrocrystallization experiments, it was necessary to verify that there was no electrochemical reaction from the substrates in the

0021-891X

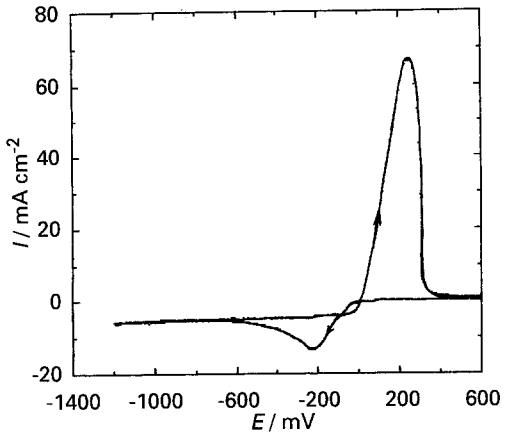

Fig. 1. Linear sweep voltammogram from copper sulphate solution at glassy carbon. Scan rate: 50 mV s^{-1}.

supporting electrolyte. Voltammograms for the two substrates used, in 0.5 M Na_2SO_4 solution without reducible cation, were traced. No electrochemical reaction was observed with glassy carbon. Figure 1 shows the voltammogram for copper electrocrystallization on GC. The cathodic part of the curve has the characteristic steep increase in current and nucleation loop of metal deposition occurring by nucleation. The hydrogen overpotential at GC is sufficiently high for copper deposition not to be affected.

The curve for the steel substrate, from a bath without copper ion, shown in Fig. 2, has a cathodic peak at −790 mV in the cathodic going scan. This peak can be attributed to the reduction of an air-formed oxide layer, because the return sweep shows no peak in this potential range. Figure 2 also shows the voltammogram for copper solution on steel, and presents two peaks in the cathodic part. The first peak, although slightly more cathodic than the nucleation peak observed with GC, shows the crossover between the cathodic and anodic going scans, characteristic of a nucleation process. The second peak is more surprising, it appears at the same potential as the reduction peak observed on steel substrate without copper ion, but is larger.

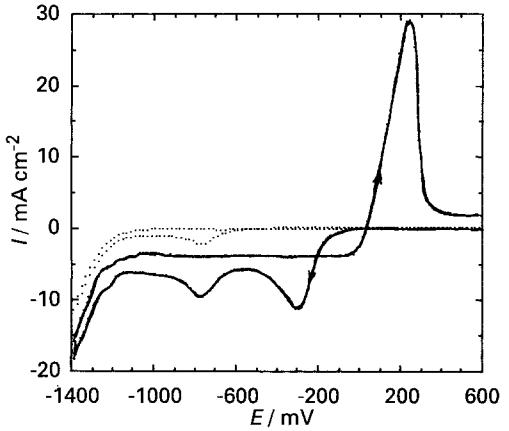

Fig. 2. Linear sweep voltammogram from sulphate solutions at stainless steel. Scan rate: 50 mV s^{-1}. Key: (···) from sulphate solution without copper species; (——) from copper sulphate solution.

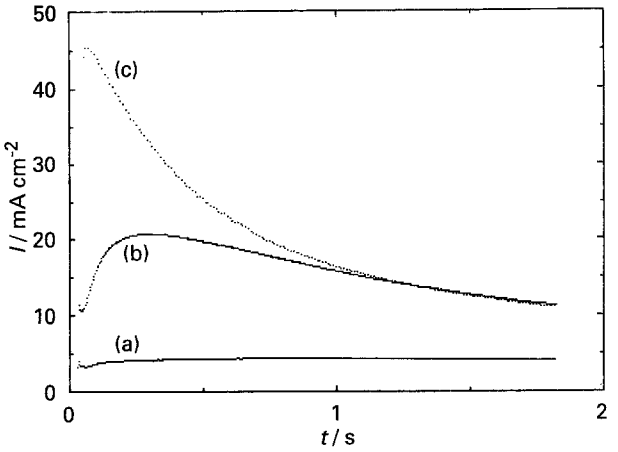

Fig. 3. Current–time transients for copper deposition on glassy carbon. Curves: (a) −100, (b) −300 and (c) −400 mV.

This peak, therefore, cannot be related only to the reduction of the air-formed oxide layer. It is likely that the peak corresponds to two simultaneous electrochemical reactions. The limiting current after the copper crystallization peak is due to the bath composition and hydrodynamic conditions; its value is identical for the two substrates.

3.2. *Potential step method*

In a series of pulse experiments, the potential was stepped from the rest potential to values determined from the corresponding voltammograms. Figure 3 presents a set of current time transients from copper solution on GC. They show an increase in current up to a maximum, which is typical for the formation of a deposit by nucleation and growth of the crystallites. The decreasing part of the transient reflects the passage to linear mass transfer; the current approaches that for linear diffusion. The logarithmic plot of the ascending part of the transient is linear. The slope of the line indicates that the current is a linear function of $t^{1/2}$, which corresponds to an instantaneous nucleation and diffusion controlled 3D growth. The transients in Fig. 3 are for two seconds, but the experiments were run for 60 s and the stabilized current reached the limiting current.

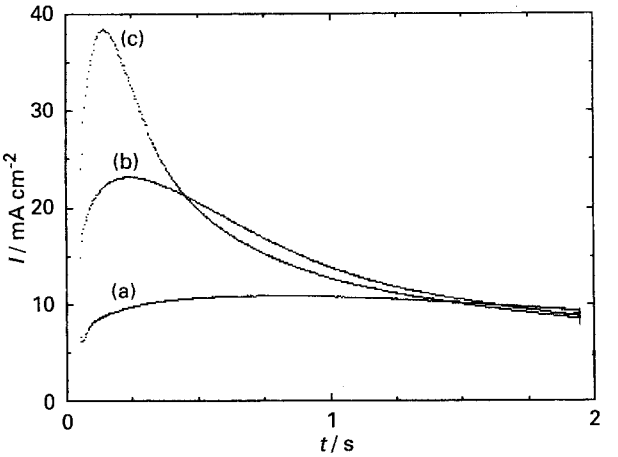

Fig. 4. Current–time transients for copper deposition on steel. Curves: (a) −300, (b) −400 and (c) −700 mV.

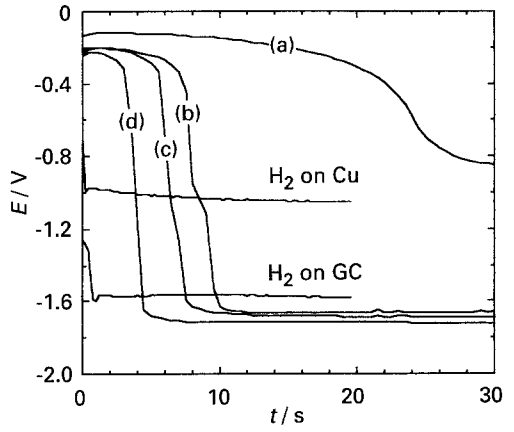

Fig. 5. Potential–time transients for copper deposition on glassy carbon. (a) 5.2; (b) 7.3; (c) 8.3 and 10.5 mA cm^{-2}.

Figure 4 presents the potential–time transients from the same solution on steel. They are similar to the transients on GC. Comparison between the transients at −400 mV for GC and steel shows that the maximum on GC is about two times higher than on steel. On steel the current rapidly reaches the limiting value. By recording the current for longer times, no other electrochemical reaction, which might be related to the second cathodic peak in the voltammogram of Fig. 2, was detected.

3.3. *Current step method*

In this study, this method was not used to study the nucleation process, since this determination is much easier by the potential step method. Galvanostatic experiments were conducted, for a relatively long time, to check the change of potential with time. Figure 5 presents the E/t transients on GC for four current densities varying from 5.2 mA cm^{-2}, which is the limiting current, up to 10.5 mA cm^{-2}. The transient for 10.5 mA cm^{-2} (curve (d)) shows two plateaux, the more anodic plateau is due to the reduction of copper cations and lasts 3 s. Curve (c) for 8.3 mA cm^{-2} has the same shape as curve (d), but a small inflection occurs between the two potential arrests. Curve (b) for 7.3 mA cm^{-2} shows a well formed arrest at about −1 V. The trace of curve (a) differs from the three others. The potential does not reach the potential of the second plateau at −1.7 V and stabilizes at −1 V. Figure 5 also shows the potential/time transients obtained from sodium sulphate solution without copper ion on GC, and on GC already coated with electrodeposited copper. On the basis of the last two transients, the potential arrest at −1 V can be related to hydrogen evolution on electrodeposited copper, and the more cathodic potential plateau to hydrogen evolution at GC. Therefore the stabilized potential for curve (a) corresponds to hydrogen evolution on copper, indicating good covering of GC by copper.

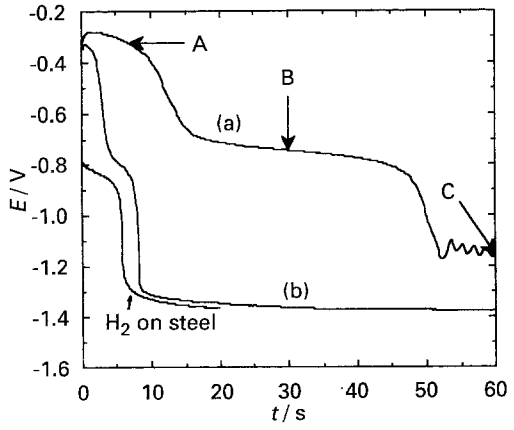

Fig. 6. Potential–time transients from copper sulphate on steel. (a) 5.2 and (b) 10.5 mA cm^{-2}.

Figure 6 presents a series of potential-time transients on steel substrate for 5.2 and 10.5 mA cm^{-2}. Curve (a) for 5.2 mA cm^{-2} exhibits three potential plateaux (A, B and C). The first plateau lasts about 10 s and its potential is in the range of the potential of the first cathodic peak observed in the voltammogram in Fig. 2. The second plateau (B) lasts longer and appears in the same potential range as the second cathodic peak in Fig. 2. The potential then stabilizes at a potential that may either be the potential of hydrogen evolution on copper or that of hydrogen evolution on steel. Figure 6 also shows the potential/time transient obtained on steel in sulphate solution without copper ion, and this curve makes it possible to choose between the two possibilities. The third plateau (C) corresponds to hydrogen evolution on copper rather than on steel; this means that the steel substrate is largely covered by copper, as seen further by microscopic examination of the deposit. Curve (b) for 10.5 mA cm^{-2} exhibits the same type of transient, but the last two plateaux are shorter. The third plateau corresponds to hydrogen evolution on steel, and therefore the substrate for this current is not well covered by copper.

Whatever the substrates, it is known that copper deposition is under mass transfer control, and the steep potential drop after the first plateau is obviously due to the depletion of copper from the diffusion layer. The product $i \times \tau^{1/2}$ (τ is the transient time of the galvanostatic response) is constant as expected for a mass transfer control. The charges under the first plateau and the $i \times \tau^{1/2}$ values obtained on GC are reported in Table 1. For 10.5 mA cm^{-2}, the charge was about 30 mC; assuming that a copper monolayer needs about 500 μC, this corresponds to about 60 monolayers. Nevertheless, as shown by the steep drop of the potential towards hydrogen evolution on GC, the substrate is not totally covered by copper. For the polarization

Table 1. Relation between current densities and charges for GC

i/mA cm^{-2}	τ/s	$i\tau^{1/2}$	Q/mC
5.2	16	20.8	83.2
7.3	8	20.6	58.4
8.3	5	18.6	41.5
10.5	3	18.2	31.5

Table 2. Relation between current densities and charges for steel

	First plateau			Second plateau		
$i/mA\,cm^{-2}$	τ/s	$i\tau^{1/2}$	Q/mC	τ/s	$i\tau^{1/2}$	Q/mC
5.2	11	17.2	57.2	45	34.9	234.0
10.5	3	18.2	31.5	9	31.5	94.5

times used, the covering of GC by copper was achieved only for $5.2\,mA\,cm^{-2}$. On steel, the first plateau also reflects mass transfer control ($i \times \tau^{1/2}$ is constant), and more surprising, the second plateau is also mass transfer controlled. The corresponding charges are reported in Table 2.

Figure 7 shows the potential–time response on steel for $5.2\,mA\,cm^{-2}$ recorded for 120 s (curve (a)). The curve for the same current density, run with stirring of the solution from the beginning of the second plateau, is also presented (curve (b)). The plateau continues for a longer time, which is typical for a deposition under mass transfer control, and this plateau therefore cannot be related only to the reduction of the air formed oxide layer on steel. Curve (a), for $5.2\,mA\,cm^{-2}$ without stirring, shows an increase in potential from the third plateau as an attempt to reach the second plateau again, followed by a decrease back to the third plateau. All these results confirm that the first two plateaux are under mass transfer control.

On steel, after nucleation similar to the nucleation of copper on GC, another process appears. The voltammogram response shows a second peak, whose potential is identical with the reduction peak of the oxide layer on steel. This peak may be related to both oxide reduction and copper deposition. The current peak in the current–time transient was followed by a monotonic decrease in current up to the limiting current, which was recorded for 60 s to check its stability. No increase in current was observed, indicating that the second cathodic peak in the voltammogram does not correspond to a nucleation process, and that it may be related to deposition occurring by a non-nucleated process. In this case there would have to be some active sites on which copper could deposit. It has been shown [7] that silver

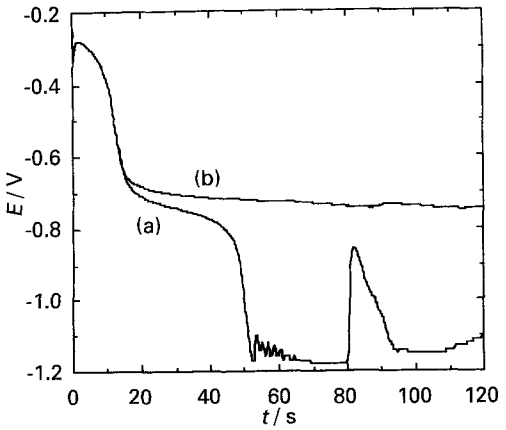

Fig. 7. Potential–time transient from copper sulphate on steel for 120 s for $5.2\,mA\,cm^{-2}$. (a) Without stirring the solution. (b) By stirring the solution from the beginning of the second plateau.

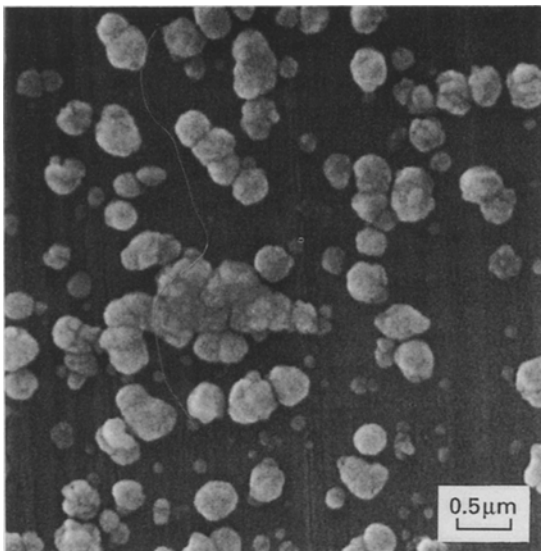

Fig. 8. Micrograph A, for copper crystallization on steel for 7 s at $5.2\,mA\,cm^{-2}$.

is deposited on platinum by non-nucleated electrodeposition on clean platinum and by nucleated electrodeposition on platinum covered by an oxide layer. The second potential plateau in the potential–time transients was diffusion controlled; therefore it cannot be related only to the reduction of an oxide layer. It thus corresponds to two simultaneous electrochemical reactions. It is likely that the reduction of the oxides was achieved during the first seconds. This lapse of time allowed the copper cations to renew the diffusion layer and allow further deposition, which explains why the plateau was longer when the solution was stirred.

These results suggest that on steel, after a first nucleation process on the air-formed oxide layer, one part of the applied current was used to reduce the air-formed oxide. Copper then deposited on the new sites formed on the substrate. These new sites allowed copper to be deposited without

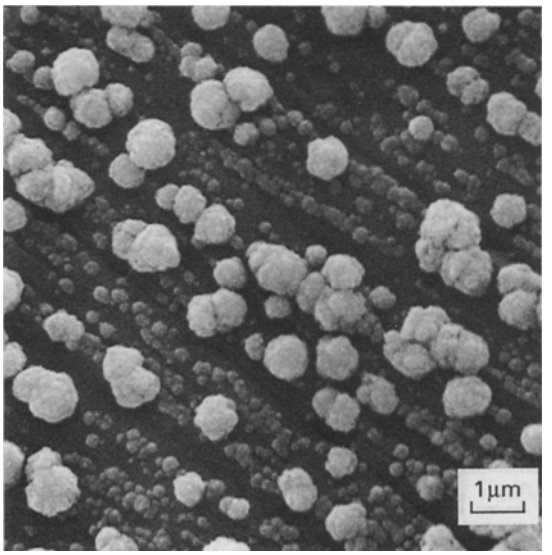

Fig. 9. Micrograph B, for copper crystallization on steel for 30 s at $5.2\,mA\,cm^{-2}$.

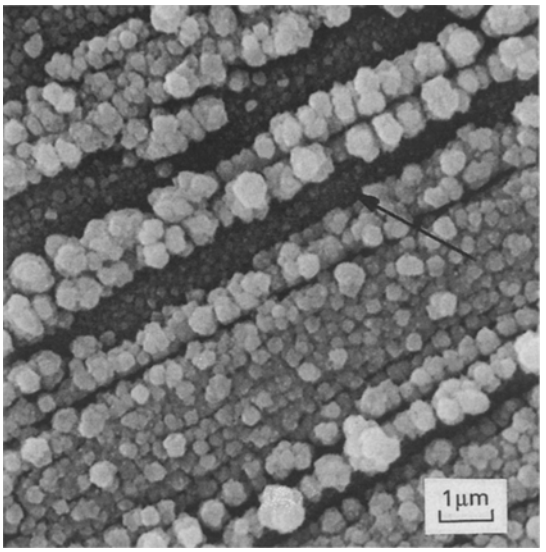

Fig. 10. Micrograph C, for copper crystallization on steel for 60 s at 5.2 mA cm^{-2}

nucleation. The substrate would then not be covered by coalescence of the first formed crystallites, as on GC substrate, but rather by non-nucleated electrodeposition on the part of the substrate left free by the first nucleated crystallites.

3.4. *Scanning electron microscopy*

A morphological study of the deposit by SEM was conducted to assess the validity of the electrochemical results. A deposit formed on GC with a 5 mA cm^{-2} current pulse for 7 s shows regular distribution of fern-shaped crystallites of similar size, which confirms the i-$t^{1/2}$ law determined from the i/t transients. For longer polarization time, the crystallites grew without forming new crystallites, which indicates instantaneous nucleation [3]. Deposits were formed on steel by pulsing at 5 mA cm^{-2} for times corresponding to arrows A, B and C in Fig. 6. For 7 s (Fig. 8) the deposit consists of spherical crystallites of similar size and a few smaller crystallites. Although the steel substrate was carefully polished with diamond powder to a mirror finish, the crystallites are more or less aligned in the same direction as the polishing lines, which may correspond to different oxidation states caused by the polishing process. Micrograph B (Fig. 9) presents both the same type of large crystallites (about twice the size of the crystallites in Fig. 8) and numerous smaller crystallites. The nucleus density of the large crystallites did not change, indicating that no new crystallites were formed from A and B potentials, and that the numerous smaller crystallites were formed at the potential of the second plateau B (Fig. 6). Micrograph C (Fig. 10) corresponds to a site where few large crystallites exist. It shows that the large crystallites are of the same size, and illustrates their alignment. Between the lines the substrate was covered by numerous smaller crystallites formed during the time corresponding to the second plateau. It is worth noting that the first crystallites did not grow further during the second potential plateau. Some parts of the substrate show still smaller crystallites, indicated by an arrow in Fig. 10. The X-ray image of this region detected iron, nickel and chromium, and therefore these crystallites resulted from the reduction of the oxides formed on the steel. For the other crystallites only copper was detected.

4. Conclusion

The initial stages of copper electrocrystallization are closely related to the substrate used. On glassy carbon, instantaneous three-dimensional nucleation and growth mechanism is observed. The crystallites formed during the first seconds grow without further nucleation; the substrate is covered by bridging of the growing crystallites. On steel, complete coverage of the substrate occurs in two stages. The first stage is the formation of copper crystallites by a 3D nucleation process on the air formed oxide layer. As the kinetics are mass transfer controlled, one part of the applied current is soon used to reduce this oxide layer, with formation of new sites for the deposition of copper by a non-nucleated process. This dual mechanism can be seen in the micrographs as two types of crystallites. Thick films are nodular on GC, and smooth with some nodular patches on steel. The galvanostatic method constitutes an interesting tool to determine the part of the substrate covered by the metallic deposit at the start of the deposition process.

References

[1] E. Chassaing and R. Wiart, *Electrochim. Acta* **29** (1984) 649.
[2] W. J. Lorenz, H. D. Hermann, N. Wüthrich and F. Hilbert, *J. Electrochem. Soc.* **121** (1974) 1167.
[3] I. Bimaghra and J. Crousier, *Mat. Chem. Phys.* **21** (1989) 109.
[4] J. Crousier and I. Bimaghra, *Electrochim. Acta* **34** (1989) 1205.
[5] P. Vanden Brande and R. Winand, *Surf. Coat. Technol.*, **52** (1992) 1.
[6] G. Gunawardena, G. Hills and I. Montenegro, *J. Electroanal. Chem.* **184** (1985) 357.
[7] G. Gunawardena, G. Hills, I. Montenegroand and B. Scharfker, *ibid.* **138** (1982) 225.